N93-27451

INVESTIGATION OF FORCED UNSTEADY SEPARATED FLOWS USING VELOCITY-VORTICITY FORM OF NAVIER-STOKES EQUATIONS

54-34
160484
10
P.

by

K. N. Ghia, U. Ghia* and G. A. Osswald

Department of Aerospace Engineering and Engineering Mechanics
*Department of Mechanical, Industrial and Nuclear Engineering
Computational Fluid Dynamics Research Laboratory
University of Cincinnati
Cincinnati, Ohio 45221

Abstract

The phenomenon of forced unsteady separation and eruption of boundary-layer vorticity is a highly-complex, high-Reynolds number flow phenomenon, which abruptly leads to the formation of a dynamic stall vortex as demonstrated earlier by the authors for a NACA 0015 airfoil undergoing constant rate pitch-up motion. This, as well as the results of other researchers, have convincingly demonstrated a complex vortical structure within the state of unsteady separation prior to the evolution of dynamic stall. This phenomenon of vortex eruption, although observed in studying dynamic stall phenomena, is also associated with transition from laminar to turbulence flow and its generic nature has been stressed by many researchers including the present investigators.

An unsteady Navier-Stokes (NS) analysis is developed for arbitrarily maneuvering bodies using velocity-vorticity variables; this formulation is nearly form-invariant under a generalized non-inertial coordinate transformation. A fully-implicit uniformly second-order (except convective terms) accurate method is used, with the nonlinear convective terms approximated using a biased third-order upwind differencing scheme to be able to simulate higher-Re flows. No explicit artificial dissipation is added. The numerical method is fully vectorized and currently achieves a computational index of 7 micro-seconds per time step per mesh point, using a single processor on the CRAY Y-MP 8/864 at the Ohio Supercomputer Center. The simulation results show that the energetic free shear from the leading edge is responsible for the wall viscous layer to abruptly erupt near the center of the counterclockwise rotating eddy in the unsteady boundary layer. Primary, secondary, tertiary and quaternary vortices have been observed before the dynamic stall vortex evolves and gathers its maximum strength. This study will discuss the simulation results of Reynolds number up to Re = 45,000 and will also discuss the effort of initial acceleration in a specific maneuver, on the evolution of the stall vortex.

NUMERICAL SIMULATIONS OF DYNAMIC STALL PHENOMENA BY DISCRETE VORTEX METHOD AND VISCOUS FLOW CALCULATION

Shigeru ASO* and Masanori HAYASHI**

* Department of Aeronautical Engineering, Kyushu University, Fukuoka, JAPAN

** Nishinippon Institute of Technology, Fukuoka, JAPAN

ABSTRACT

Dynamic stall phenomena have been simulated numerically by a discrete vortex method and viscous flow calculations. Both simulations could capture the characteristics of dynamic stall phenomena qualitatively. Also some numerical results show good agreements with experiments.

In the calculations by a discrete vortex method combined with a panel method the potential flows around wing sections is expressed by vortex sheets and separated shear layers are expressed by discrete vortices. Separated flows around pitching airfoils(NACA0012) are simulated for various conditions. A hysteresis of lift of airfoil at dynamic stall is obtained. The results suggest that the method has a excellent capability of simulating vortical flows with excellent small computation cost. In the calculations by viscous flow calculations incompressible Navier-Stokes equations have been solved by a third-order upwind scheme in order to understand the flow structure and mechanism of dynamic stall. Especially the flow mechanics of movement of separation point on the wing surface, vortex formation from the surface of the wing and unsteady Kutta conditions at the trailing edge of the wing are investigated carefully. The unsteady flow fields around a pitching airfoil are calculated by moving a grid system relative to the freestream. Remarkable characteristics of dynamic stall are obtained. Also the hysteresis curve of aerodynamic characteristics of C_L and C_M are obtained.

1. INTRODUCTION

Studies on dynamic stall have been conducted experimentally and theoretically by the many researchers[1-5]. However as the phenomena are essentially non-linear and the flow field becomes complicated as the separated region is increased, those phenomena are not understood sufficiently.

In this paper two efforts for simulating dynamic stall phenomena are discussed. One is based on a discrete vortex method combined with a panel method and the other is based on viscous flow calculations. Both simulations could capture the qualitative properties on dynamic stall phenomena. Also some numerical results show good agreements with experiments.

In the calculations by a discrete vortex method combined with a panel method[e.g.6] the potential flows around wing sections is expressed by vortex sheets and separated shear layers are expressed by discrete vortices. For the calculations a new numerical scheme developed by the present authors[7] have been used. In the calculation a wing section is expressed by a set of linearly distributed vortex sheets and the separation points are determined by boundary layer calculations. Separated flows around pitching airfoils are simulated for various conditions. A hysteresis of lift of airfoil at dynamic stall is obtained. The results suggest that the method has a excellent capability of simulating vortical flows with excellent small computation cost.

In the calculations by viscous flow calculations incompressible Navier-Stokes equations have been solved by a third-order upwind scheme in order to understand the flow structure and mechanism of dynamic stall. Especially the flow mechanics of movement of separation point on the wing surface, vortex formation from the surface of the wing and unsteady Kutta condition at the trailing edge of the wing are investigated carefully. The unsteady flow fields around a pitching airfoil are calculated by moving a grid system relative to the freestream. Remarkable characteristics of dynamic stall are obtained. Also the hysteresis curve of aerodynamic characteristics of C_L and C_M are obtained.

2. Numerical Simulation of Dynamic Stall by Discrete Vortex Method

2.1 Analytical Method

The complex potential f of the flow field is expressed by the following form:

$$f = Ue^{-i\alpha}z + i\int_B \frac{\gamma(\zeta)}{2\pi} log(z-\zeta)d\zeta$$

$$+i\sum_{k=1}^{M}\left(\frac{\Gamma_{Ak}}{2\pi}log(z-z_{Ak}) + \frac{\Gamma_{Bk}}{2\pi}log(z-z_{Bk})\right) \qquad (1)$$

, where U is the uniform flow velocity and α is the angle of attack. The discrete vortices expressing separated shear layers are shed from the separation points on the wing surface. The circulation of each vortex is estimated using the velocity at the point assumed as the edge of the boundary layer near the separation point. Hence, unknown quantities in the flow field are the amount of strength of the singular points on the wing surface and solved at each time step by using boundary condition for normal velocity through the control point on the surface. The detailed description of the method are discussed in Ref. 7.

For the calculation of the flow around the pitching wing section, incident angle of the freestream is sinusoidally changed. Then the angle of attack of the wing section is given by following form:

$$\alpha = \alpha_0 + \alpha_1 sin\omega t \tag{2}$$

, where the angular frequency ω is related to the reduced frequency k by the following form:

$$k = \frac{\omega c}{2U_\infty} \tag{3}$$

where c is the chord length. As the separation point on the wing section is not obvious a priori, the separation point is determined by the boundary layer calculations. The Thwaites' method[e.g.6] is used for the laminar boundary layer calculation and the Truckenbrodt's method[e.g.8] is used for the turbulent boundary layer calculation.

2.2 Separated Flows around a Wing Section at a Fixed Angle of Attack

Fig. 1 shows sevral calculated instantaneous stream lines around a wing section of NACA4412 at angle of attack of 20 degrees. As shown in the Figure the flow is quite unsteady and the changes of separation point and separated region can be observed. The calculated pressure distribution is compared with the experiments in Fig. 2. As shown in the Figure the calculated pressure distribution shows good agreement with that by experiment[9] including the separated region. Fig. 3 shows C_L and C_D with α. A good agreement of C_L between the calculations and the experiments is obtained. Also the results of C_D show good agreement with the experiments. Those results suggest that a discrete vortex method is quite powerful for prediction of aerodynamic characteristics of a wing section at static angle of attack.

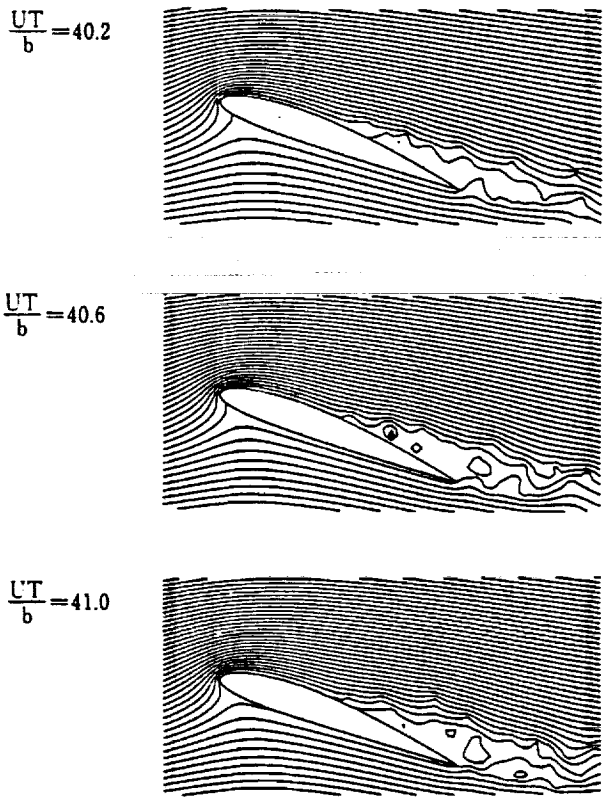

Fig. 1 Instantaneous stream lines(NACA4412, α = 20*degrees*, $Re = 1.0 \times 10^6$)

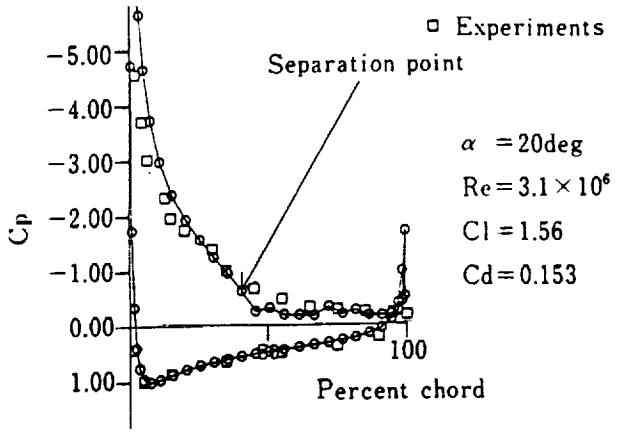

Fig. 2 Comparison of pressure distribution with experiments(NACA4412, $\alpha = 20degrees$, $Re = 1.0 \times 10^6$)

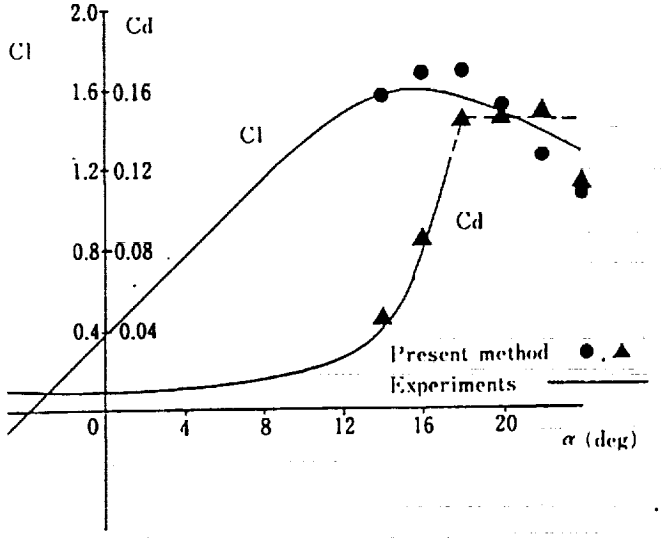

Fig. 3 Comparision of C_L and C_D with experiments

2.3 Separated Flows around an Oscillating Wing Section in Pitch

The calculated results of separated flows around pitching airfoil(NACA0012) under the condition of $\alpha = 15^0 + 10^0 sin\omega t (k = 0.15)$ and Reynolds number=1.0×10^6 is shown in Fig. 4. As shown in the figure separated region is small in pitching-up process and it becomes much larger in pitching-down process. Quite different characteristics of flow patterns between in pitching-up and pitching-down processes are obtained. The results show some features of dynamic stall. The calculated aerodynamic characteristics are compared with experiments[1] as shown in Fig. 5. The calculated Hysteresis curve of C_L show almost same tendency as the experiments. The results show fairly good agreements with experiments.

Another calculation have been conducted under the condition of $\alpha = 15^0 + 14^0 sin\omega t (k = 0.1)$ and Reynolds number=1.0×10^6 as shown in Fig. 6. In the Figure separated region is small in pitching-up process and it becomes much

larger in pitching-down process. Quite different characteristics of flow patterns between in pitching-up and pitching-down processes are also obtained. The calculated aerodynamic characteristics are compared with experiments[1] as shown in Fig. 7. The calculated Hysteresis curve of C_L show almost same tendency as the experiments. The results show fairly good agreements with experiments qualitatively. The results show C_L of oscillating airfoil shows higher maximum value compared with that of a stationary airfoil.

Those calculated results show qualitatively good agreement with experiments and excellent capability of the method is proved. Also as the computation time for each calculation is quite small compared with those of other finite-difference methods, the method is quite useful for the first estimation of the aerodynamic characteristics of a new wing section.

3. Numerical Simulation of Dynamic Stall by Viscous Flow Calculation

3.1 Numerical Procedures

Unsteady flows of viscous incompressible fluid flow around a airfoil is considered. The governing equations are equations of continuity and incompressible Navier-Stokes equations:

$$\mathrm{div}\boldsymbol{V} = 0 \tag{4}$$

$$\frac{\partial \boldsymbol{V}}{\partial t} + (\boldsymbol{V}\cdot\nabla)\boldsymbol{V} = -\mathrm{grad}\, p + \frac{1}{Re}\Delta \boldsymbol{V} \tag{5}$$

where Re is Reynolds number. Following MAC method (Marker and Cell method)[10], the Poisson equation for the pressure p is derived by taking divergence of Eq(5):

$$\Delta p = -\mathrm{div}(\boldsymbol{V}\cdot\nabla)\boldsymbol{V} + R \tag{6}$$

where

$$R = -\frac{\partial D}{\partial t} + \frac{1}{Re}\Delta D\ , \qquad D = \mathrm{div}\boldsymbol{V} \tag{7}$$

Although R in Eq.(7) is identically zero due to Eq.(1), it is retained here as a corrective term in order to prevent the accumulation of numerical errors. If $\boldsymbol{V}$ is given at certain time, then the Poisson equation (6) can be solved to get p, and then by substituting these value into Eq.(5), $\boldsymbol{V}$ at next time is calculated from Eq.(5). The detailed numerical procedures will be given in Reference 11.

For mesh grid generation Steger and Sorenson's method[12] is used. The method is useful to generate a body-fitted mesh system for an arbitrary body with keeping almost orthogonal coordinates system at the wall. The mesh system is generated as O-grid type and quite fine mesh is prepared in the vicinity of the body surface. For the calculation of separated flow around oscillating airfoil a general coordinate system with time-dependent variables is introduced. However in the computation using those coordinate systems the displacement of the grid point and distortion of the mesh system for each time interval should be considered carefully. In the present computation the method proposed by Nakamichi[13] is used.

In the velocity fields non-slip conditions are used for the wing surface and uniform flow conditions are used for outer boundary. In the pressure fields zero derivative normal to the wing surface is used and zero derivative parallel to the freestream is used at exit boundary.

3.2 Separated Flows around an Airfoil at Fixed Attack Angle

Before the calculations the preliminary calculation has been conducted for separated flows around circular cylinder at low Reynolds number in order to check the validity of the numerical scheme by the present authors[14]. The results show excellent agreements with experiments. The width of the separated region and flow patterns are predicted quite precisely. The results show the present numerical scheme is quite useful and reliable for incompressible viscous flow.

The mesh system(85 x 61) generated for a wing section of NACA0012 is shown in Fig. 8. Quite fine mesh is prepared in the vicinity of the wing surface and quite wide range of outer boundary are considered. The separated flows around airfoil at various attack angle is calculated at Reynolds number of 300. The representative results of in-

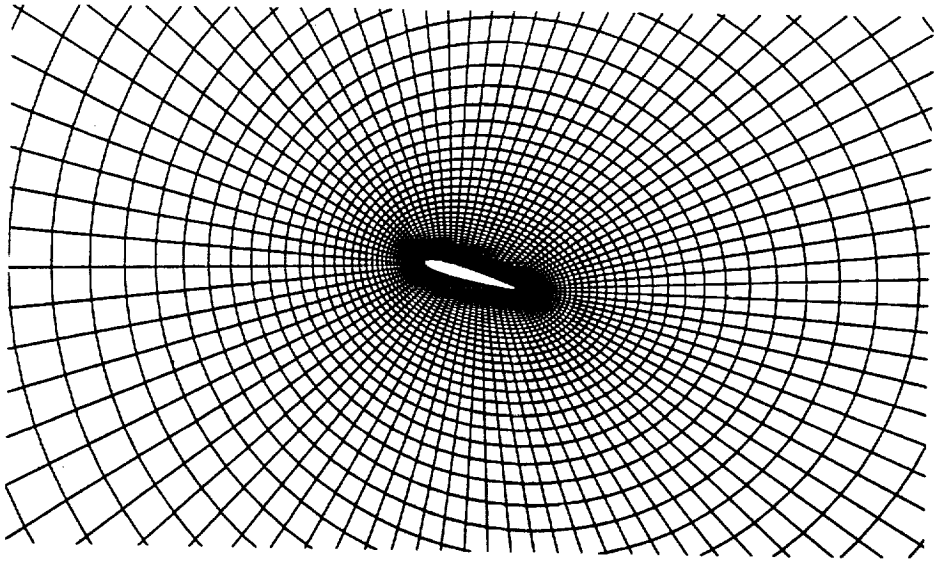

Fig. 8 Mesh system (NACA0012;IMAX=85, JMAX=61)

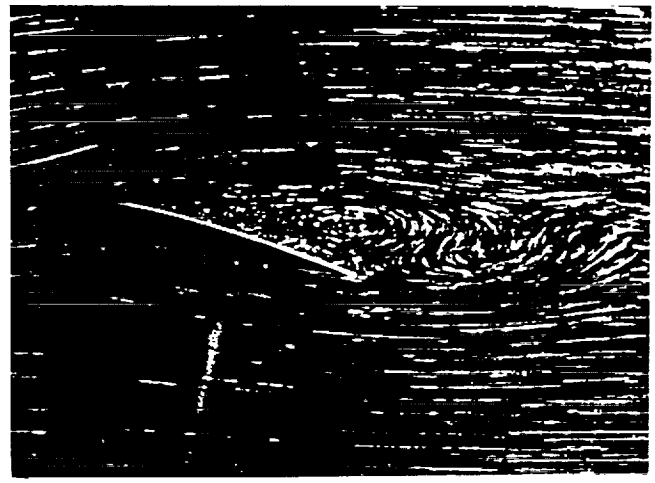

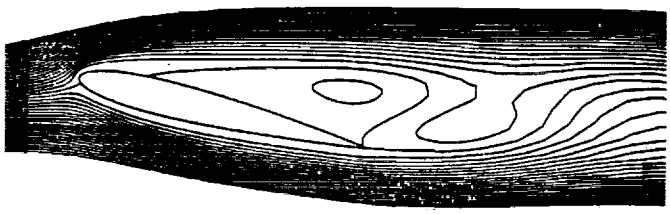

(a) $\alpha = 14^0$

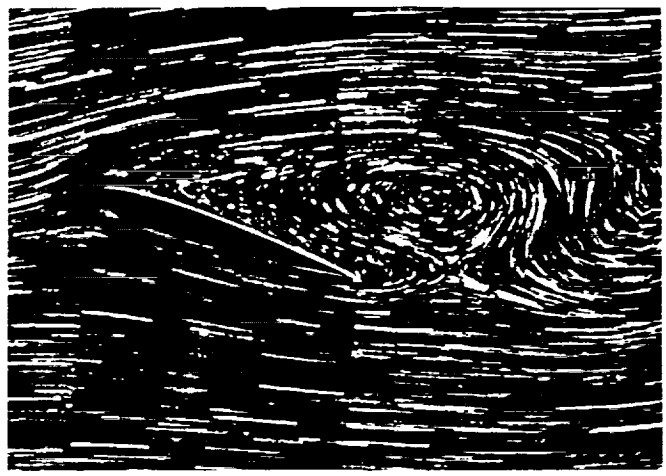

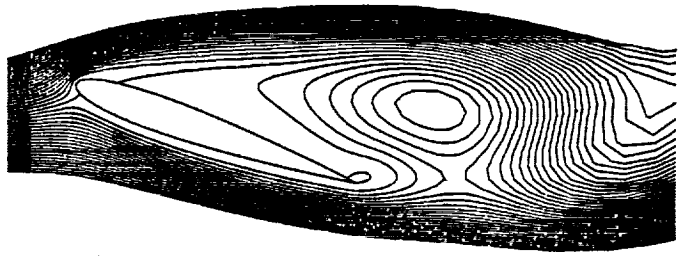

(c) $\alpha = 20^0$

Fig. 9 Comparison of Flow patterns(instantaneous stream lines) between calculations and experiments(Aluminum powder) (NACA0012; Re=300)

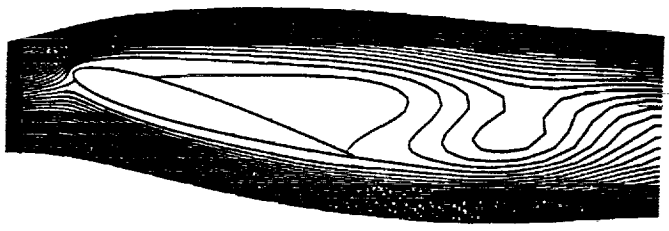

(b) $\alpha = 16^0$

Fig. 10 Comparison of flow patterns(electrolytic precipitation pictures) between calculations and experiments (NACA0012; Re=300, $\alpha = 20^0$)

stantaneous stream lines are compared with experimental results obtained by the present authors as shown in Fig. 9. The results show excellent agreements with experiments at various attack angle. As shown in the Figures separated region become large as attack angle is increased. In the present conditions separated shear layer forms a vortex and convects in the freestream. Karman vortex shedding pattern is observed behind an airfoil section. A separated shear layer shed from the trailing edge forms another vortex and rolls up behind a airfoil and convects downstream. The flow is quite periodic and those flow patterns repeat at every interval.

The separated flow patterns can be also visualized by the electrolytic precipitation method. Fig. 10 shows comparison of calculated electrolytic precipitation picture and that obtained by the experiments. In the calculation numerous marker particles are introduced in the vicinity of the airfoil surface at some time interval and their temporal traces, which are induced by the velocity fields, are calculated. Those traces form streak lines of the flow fields. A Crank-Nicolson's implicit time integration is used in order to get accurate temporal resolution. The results show the numerical streak lines , i.e. numerical electrolytic precipitation pictures, is quite useful in order to understand the structure of the flow fields and compare the calculated results with experiments.

3.3 Separated Flows around an Oscillating Airfoil in Pitch

In the previous section the numerical scheme used in the present calculation is proved to be quite useful and reliable, the unsteady flow fields around a oscillating airfoil in pitch are calculated by moving a grid system relative to the freestream. The flow conditions are selected from the experiments conducted by the present authors. The center of rotation is located at 25 percent of the chord and an airfoil section of NACA0012 is oscillated sinusoidally in pitch at reduced frequency of $k = \omega c/2U = 0.2$ and Reynolds number of 7.0×10^4. c is a chord length and U is freestream velocity.

The representative calculated results under the condition of $\alpha = 12^0 + 4^0 sin\omega t$, $k = 0.2$ and Reynolds number=7.0×10^4 is shown in Fig. 12. Instantaneous stream lines and numerical smoke wire diagrams are shown in the Figures. For the calculations of numerical smoke-wire picture numerous fluid particles are introduced at equi-spacing points along a perpendicular axis, which is set in front of an airfoil for several time interval and their temporal traces, which are induced by the velocity fields, are calculated. Those traces form streak lines and a numerical smoke-wire picture is obtained. A Crank-Nicolson's implicit time integration is used

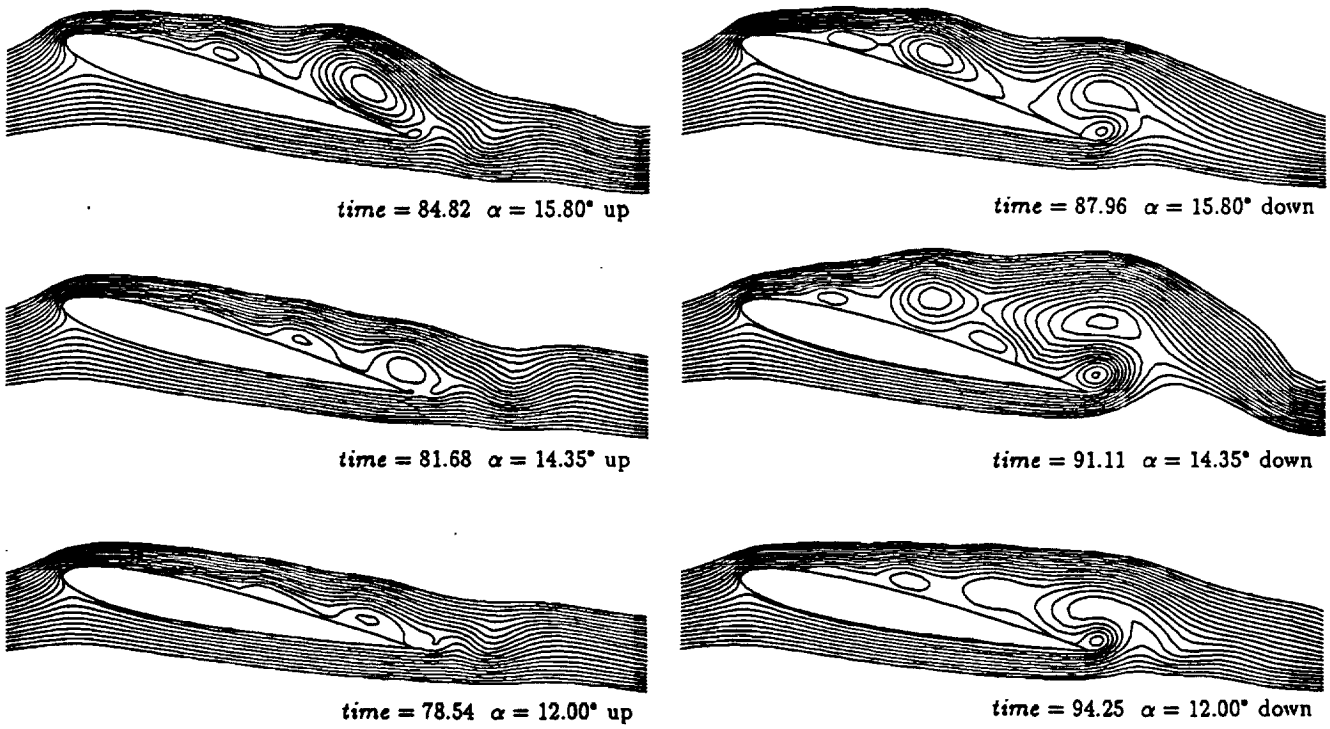

(a) Instantaneous stream lines

Fig. 11 Calculated flow patterns(NACA012, $\alpha = 12^0 + 4^0 sin\omega t (k = 0.2), Re = 7.0 \times 10^4$)

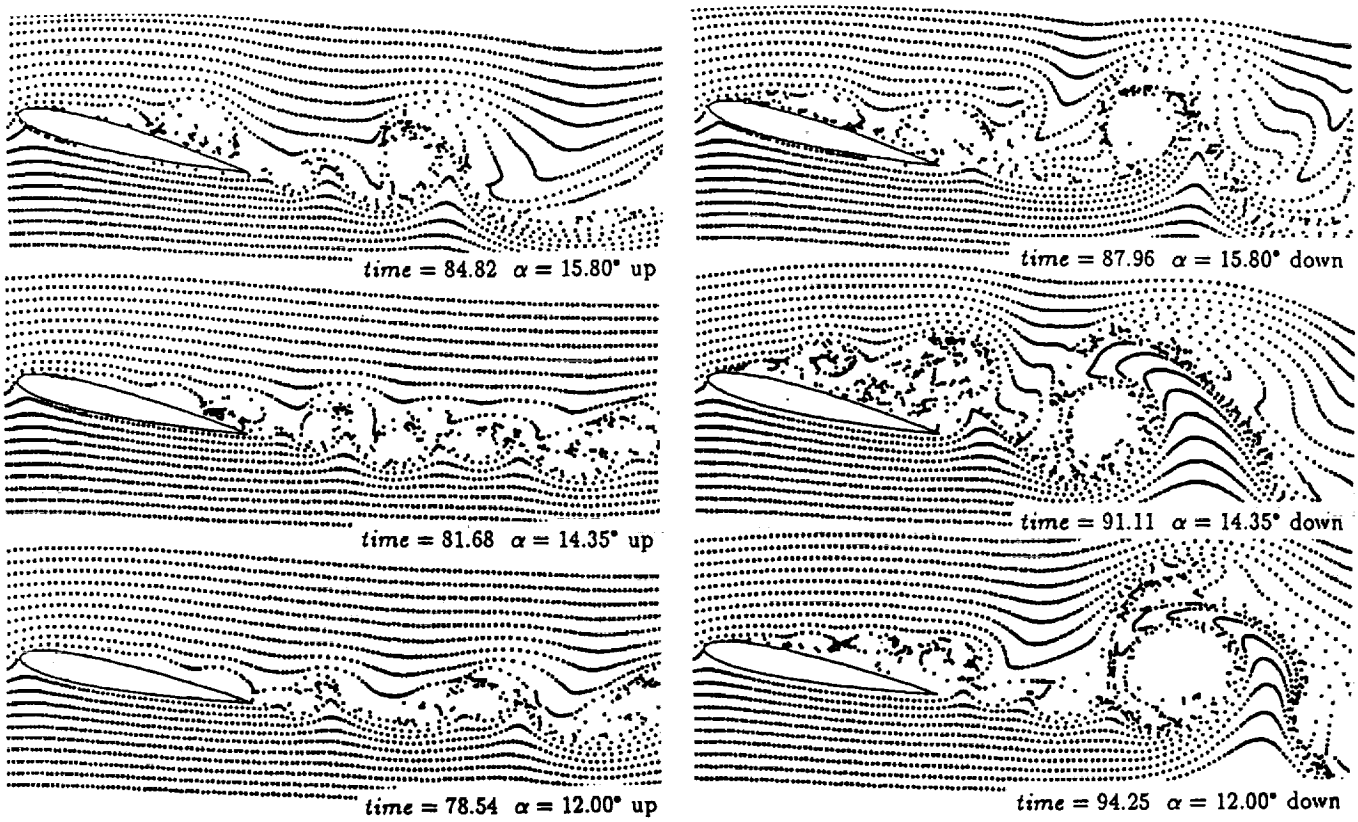

Fig. 11 (b) Numerical smoke-wire picture

in order to get accurate temporal resolution. The results show the numerical smoke-wire pictures are quite useful in order to understand the structure of the flow fields and compare the calculated results with experiments.

As shown in the figure separated region is small in pitching-up process and it becomes large in pitching-down process. Quite different characteristics of flow patterns between in pitching-up and pitching-down processes are obtained. The significant change of the flow patterns in pitching-up and pitching-down process show the existence of the Hysteresis of the aerodynamic characteristics. The hysteresis curve of aerodynamic characteristics of C_L and C_M at the same condition are shown in Fig. 13. In particular C_L at higher attack angle than the stalling angle of this airfoil section keeps higher value, then decreases rapidly. The results shows remarkable characteristics of dynamic stall.

4. CONCLUSIONS

Dynamic stall phenomena have been simulated numerically by a discrete vortex method and viscous flow calculations and major results of using both numerical efforts are discussed. The major conclusions of the present study are summarized as follows:

In the calculations by a discrete vortex method combined with a panel method the potential flows around wing sections aerodynamic characteristics of dynamic stall is calculated properly and a hysteresis of lift of airfoil at dynamic stall is obtained. The results suggest that the method has a excellent capability of simulating vortical flows with excellent small computation cost.

In the calculations by viscous flow calculations separated flows around oscillating airfoil in pitch are simulated by using the third-order upwind scheme and a moving mesh system. The calculated separated region is small in pitching-up process and it becomes large in a pitching-down process. Quite different characteristics of flow patterns between in a pitching-up and pitching-down processes and hysteresis curve of aerodynamic characteristics are obtained.

ACKNOWLEGEMENT

The present authors would like to express thier cordial gratitude to Mr. Naoki FUTATSUDERA, Mr. Atsushi FUJIMOTO and Mr. Atsuhiro SAKAMOTO for thier valuable support in the present study during thier stay in our laboratory.

REFERENCES

1) McCrosky, W. J. and Pucci, S.L.: Viscous-Inviscid Interaction on Oscillating Airfoils, AIAA paper 81-0051 (1981).
2) McCrosky, W. J.: Unsteady Airfoils, Ann. Rev. Fluid Mech., 14 (1982), pp.285-311.
3) Aihara, Y., Koyama, H. and Murashige, A.: Transient Aerodynamic Characteristics of a Two-Dimensional Airfoil During Stepwise Incidence Variation, J. Aircraft, 2 (1985), pp.661-668.
4) Carr, L. W.: Progress in Analysis and Prediction of Dynamic Stall, J. Aircraft, 25 (1988), pp.6-17.
5) Oshima, K and Oshima, Y.: Flow Simulation by Discrete Vortex Method, Proc. 8th ICNMFD (1982), pp.94-106.

6) Sakata, H., Adachi, K. and Inamuro, R.: A numerical method of unsteady flows with separation by vortex shedding models(Part 1), J. Japan Society of Mechanical Engineering, 49B (1983), pp.801- 808.(in Japanese).
7) Aso, S., Hayashi, M. and Futatsudera, N.: Numerical Simulation of Separated Flows around Two-Dimensional Wing Section by a Discrete Vortex Method, Proc. Symp. on Mechanics for Space Flight 1988 of ISAS (1988), pp.11-20.
8) Hayashi, M. and Endo, E.: Measurement of Flow Fields around an Airfoil Section with Separation, Transaction of the Japan Society for Aeronautics and Space Sciences, 21 (1978), pp.69-75.
9) Schlichiting, H.: Boundary Layer Theory(7th ed.), McGraw-Hill (1979).
10) Harlow, F. H. and Welch, J. E.: Numerical Calculation of Time- Dependent Viscous incompressible Flow of Fluid with Free Surface, Phys. Fluid, 8 (1965).Phys. Fluid, 8 (1965).
11) Kawamura, T. and Kuwahara, K.: Computation of High Reynolds Number Flow around a Circular Cylinder with Surface Roughness, AIAA paper 84-0340 (1984).
12) Steger, J. L. and Sorenson, R. L.: Automatic Mesh-Point Clustering near a Boundary in Grid Generation with Elliptic Partial Differential Equation, J. Computational Physics, 33 (1979), pp.405-410.
13) Nakamichi, J.: Calculations of Unsteady Navier-Stokes Equations around an Oscillating 3-D Wing Using Moving Grid System, AIAA paper 87-1158 (1987).
14) ASO, S. and SAKAMOTO, A.: A Numerical Simulation of Separated Flows around Bodies, Technology Reports of Kyushu University, Vol.64, No. 4 (1991), pp.249-255 (in Japanese).

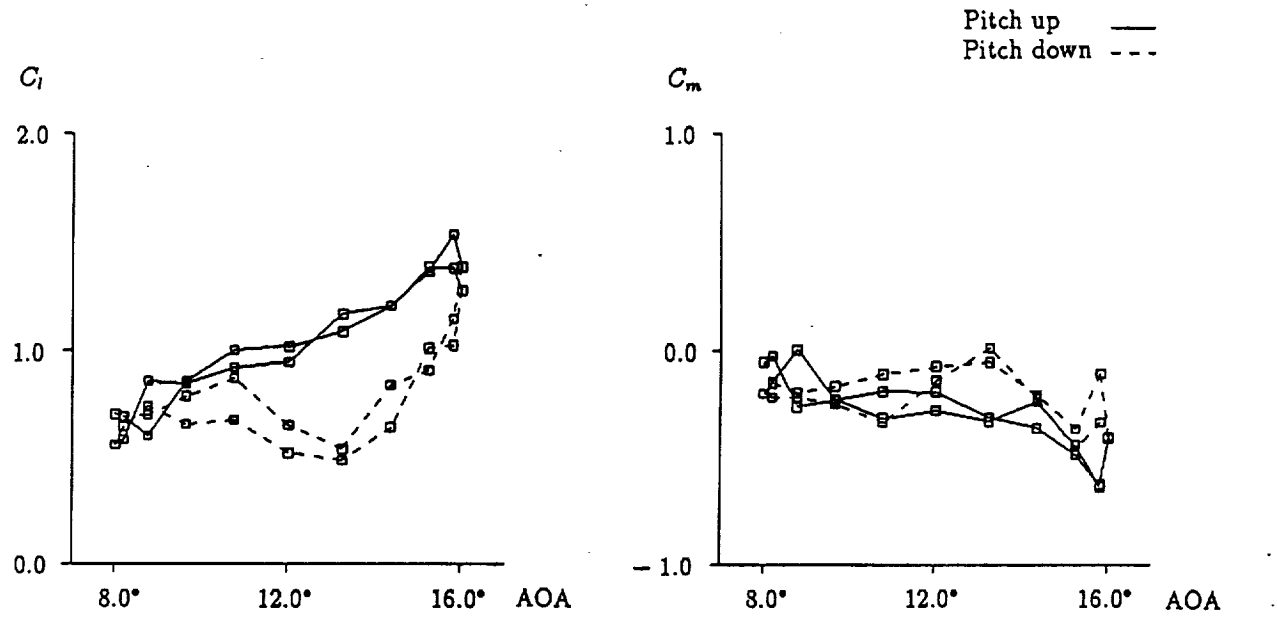

Fig. 12 The hysteresis curves of aerodynamic characteristics of C_L and C_M (NACA012, $\alpha = 12^0 + 4^0 sin\omega t (k = 0.2), Re = 7.0 \times 10^4$)

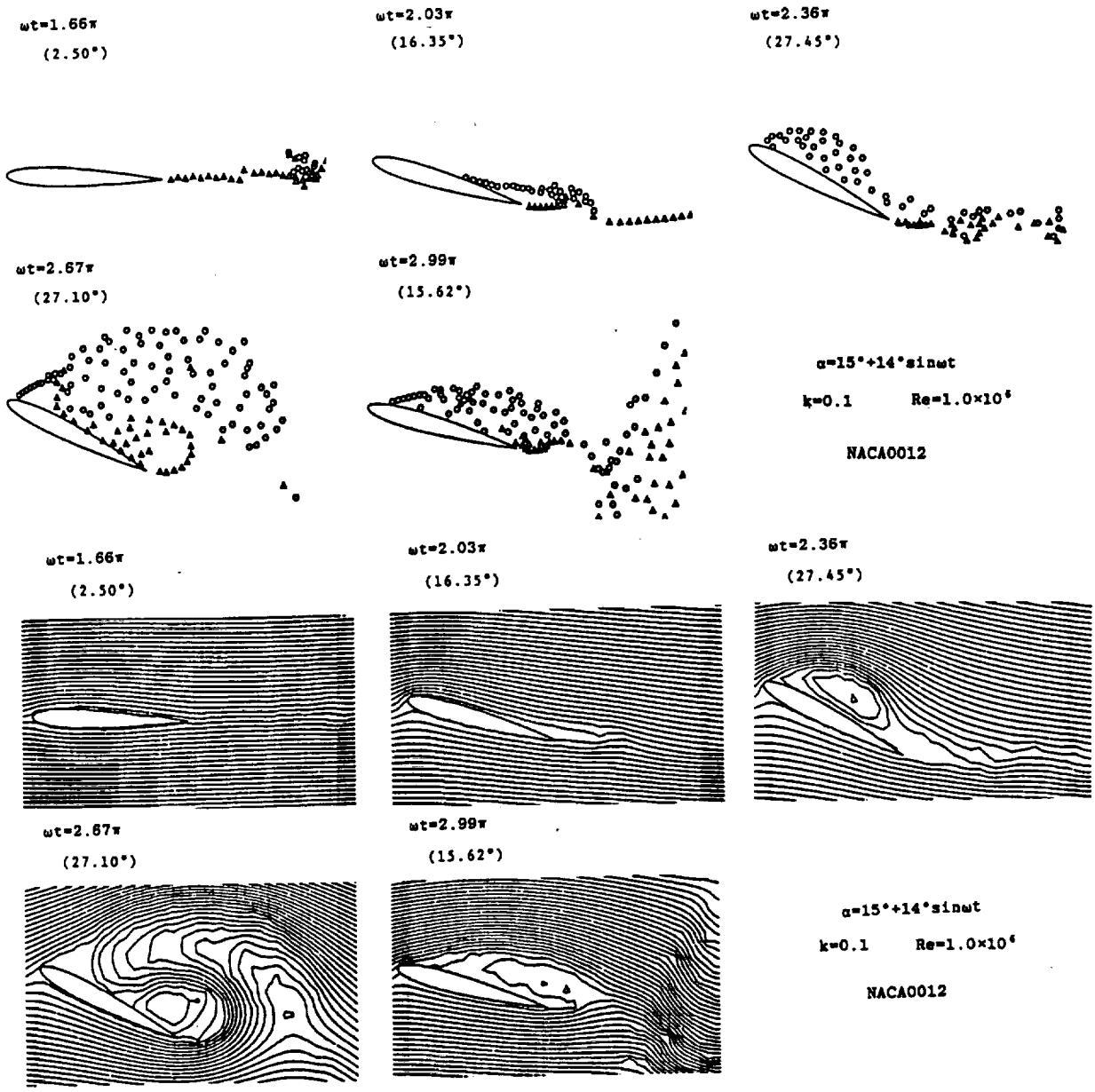

Fig. 6 Flow patterns at $\alpha = 15^0 + 14^0 sin\omega t (k = 0.1$; NACA0012, $Re = 1.0 \times 10^6)$

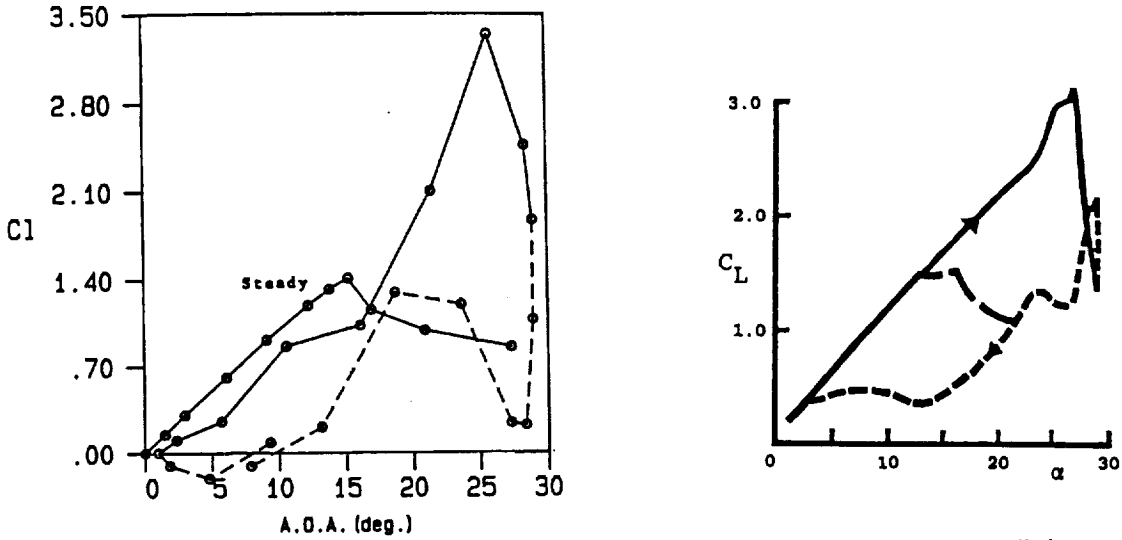

Fig. 7 Comparisons of calculated hysteresis curves of C_L with experiments[1] ($\alpha = 15^0 + 14^0 sin\omega t (k = 0.1$; NACA0012, $Re = 1.0 \times 10^6)$)

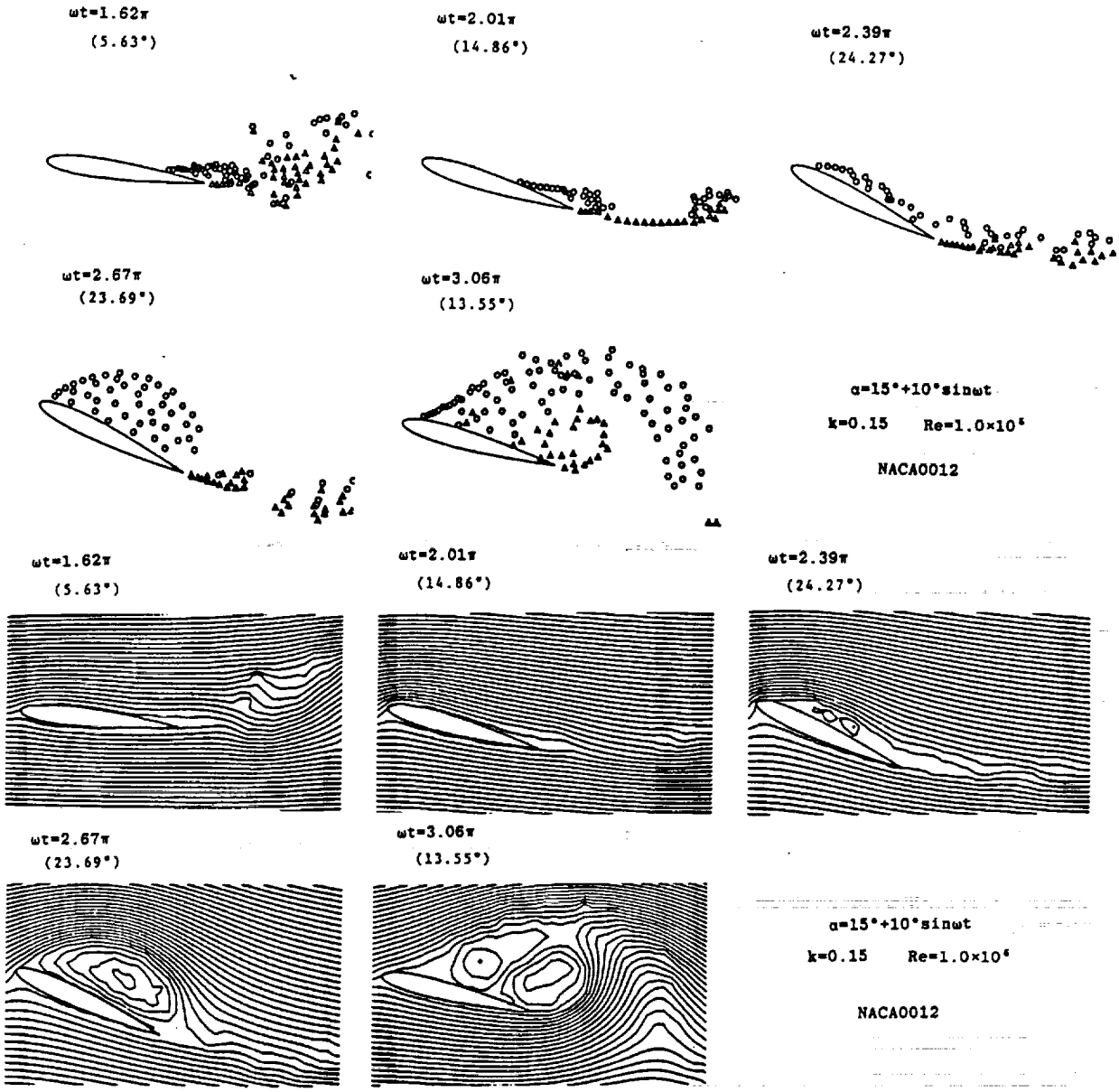

Fig. 4 Flow patterns at $\alpha = 15^0 + 10^0 sin\omega t (k = 0.15$; NACA0012, $Re = 1.0 \times 10^6)$

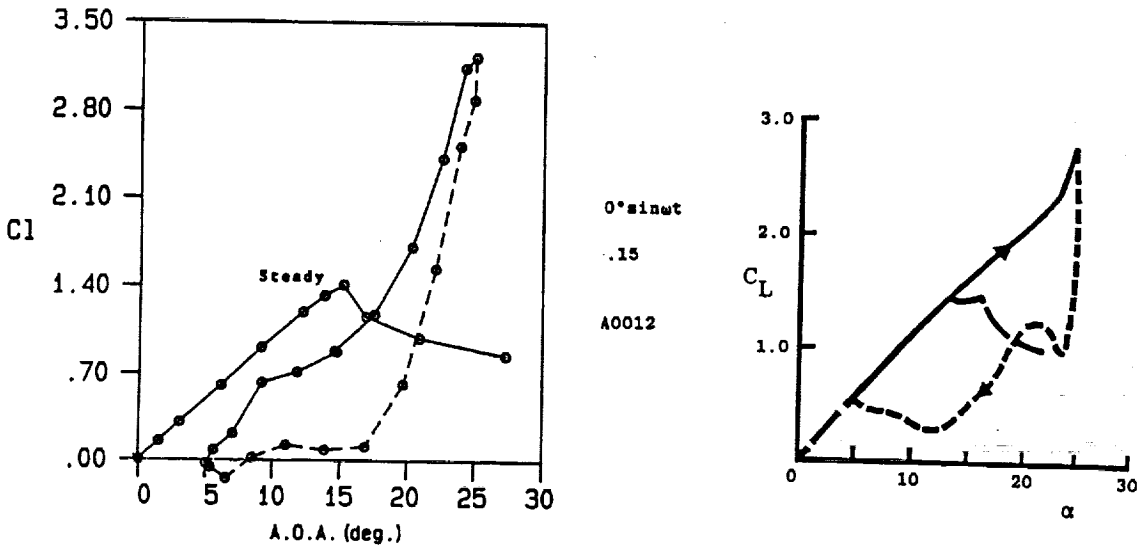

Fig. 5 Comparisons of calculated hysteresis curves of C_L with experiments[1] ($\alpha = 15^0 + 10^0 sin\omega t (k = 0.15$; NACA0012, $Re = 1.0 \times 10^6)$)